

Metabolic engineering of a carbapenem antibiotic synthesis pathway in *Escherichia coli*

Shomar, Helena; Gontier, Sophie; van Den Broek, Niels J.F.; Tejada Mora, Héctor; Noga, Marek J.; Hagedoorn, Peter Leon; Bokinsky, Gregory

DOI

[10.1038/s41589-018-0084-6](https://doi.org/10.1038/s41589-018-0084-6)

Publication date

2018

Document Version

Final published version

Published in

Nature Chemical Biology

Citation (APA)

Shomar, H., Gontier, S., van Den Broek, N. J. F., Tejada Mora, H., Noga, M. J., Hagedoorn, P. L., & Bokinsky, G. (2018). Metabolic engineering of a carbapenem antibiotic synthesis pathway in *Escherichia coli*. *Nature Chemical Biology*, 1-7. <https://doi.org/10.1038/s41589-018-0084-6>

Important note

To cite this publication, please use the final published version (if applicable).
Please check the document version above.

Copyright

Other than for strictly personal use, it is not permitted to download, forward or distribute the text or part of it, without the consent of the author(s) and/or copyright holder(s), unless the work is under an open content license such as Creative Commons.

Takedown policy

Please contact us and provide details if you believe this document breaches copyrights.
We will remove access to the work immediately and investigate your claim.

Metabolic engineering of a carbapenem antibiotic synthesis pathway in *Escherichia coli*

Helena Shomar¹, Sophie Gontier², Niels J. F. van den Broek¹, Héctor Tejeda Mora¹, Marek J. Noga¹, Peter-Leon Hagedoorn³ and Gregory Bokinsky^{1*}

Carbapenems, a family of β -lactam antibiotics, are among the most powerful bactericidal compounds in clinical use. However, as rational engineering of native carbapenem-producing microbes is not currently possible, the present carbapenem supply relies upon total chemical synthesis of artificial carbapenem derivatives. To enable access to the full diversity of natural carbapenems, we have engineered production of a simple carbapenem antibiotic within *Escherichia coli*. By increasing concentrations of precursor metabolites and identifying a reducing cofactor of a bottleneck enzyme, we improved productivity by 60-fold over the minimal pathway and surpassed reported titers obtained from carbapenem-producing *Streptomyces* species. We stabilized *E. coli* metabolism against antibacterial effects of the carbapenem product by artificially inhibiting membrane synthesis, which further increased antibiotic productivity. As all known naturally occurring carbapenems are derived from a common intermediate, our engineered strain provides a platform for biosynthesis of tailored carbapenem derivatives in a genetically tractable and fast-growing species.

New antibiotics are critically needed in the fight against antimicrobial resistance. Though metagenome sequences¹, difficult-to-culture organisms² and cryptic biosynthetic gene clusters³ have been successfully mined for novel antibiotics, such compounds are often produced at titers far too low for large-scale production^{2,4} or biochemical characterization³. Prior to the arrival of modern genetic engineering methods, the use of fermentation engineering and untargeted mutagenesis yielded strains capable of large-scale antibiotic production. Unfortunately, these techniques do not guarantee higher titers^{5–7} and cannot be applied to microbial species that cannot be cultivated in the laboratory². Furthermore, improving production by rational metabolic engineering is either intractably slow or not yet possible for most species⁸. Thus, without a platform for high-titer production, many antibiotics will remain beyond our reach and thus clinically irrelevant. Developing new platforms for antibiotic synthesis (for example, heterologous hosts or novel production methods) is therefore as urgent as discovering new antibiotics and biosynthetic pathways.

The use of fast-growing, genetically tractable species (such as *E. coli*⁹ and *Saccharomyces cerevisiae*⁹) as heterologous hosts for antibiotic biosynthesis could bridge discovery with production. The immense wealth of genetic tools available for such hosts enables rapid design and testing of engineered pathways. Improved pathways could be reintroduced into native antibiotic producers when possible⁵, or large-scale production could be further developed using the heterologous host. Heterologous production is likely the only solution for harnessing biosynthesis pathways from uncultivable organisms such as sponge symbionts¹⁰. Heterologous expression could also enable the generation of novel antibiotic derivatives (via in vivo combinatorial biochemistry or enzyme engineering¹¹). However, any attempt to engineer heterologous production, especially within susceptible bacterial species, must address the effects of the antibiotic on the host. This is especially true for bactericidal antibiotics, which cause cell death, disrupt metabolism and arrest

antibiotic synthesis. Although bacteriostatic (growth-arresting) antibiotics such as erythromycin have been produced using *E. coli*¹², its suitability for production of small-molecule bactericidal antibiotics at high titers has not yet been systematically explored.

The carbapenems, a family of β -lactams, exemplify a class of bactericidal antibiotics that currently must be chemically synthesized because of difficulties improving production by natural microbial hosts. Carbapenems are relied upon as last-resort treatments against multidrug-resistant infections¹³ and are particularly valuable because of their broad-spectrum activity and superior resistance against the vast majority of β -lactamase enzymes¹⁴. However, bacterial resistance to carbapenems is rapidly increasing owing to the proliferation of genes encoding specific metallo- β -lactamases active against carbapenems¹⁵. Carbapenem resistance could be addressed using the more than 40 naturally occurring known carbapenems if large-scale production of such compounds was possible. Unfortunately, carbapenem titers from microbial production are typically low (for example, 1–4 mg/L thienamycin from wild-type *Streptomyces cattleya*)¹⁶, and a lack of sophisticated genetic engineering tools has precluded extensive metabolic engineering of native hosts⁸. Engineering carbapenem production within heterologous hosts that are more genetically tractable could circumvent this obstacle and accelerate deployment of natural and novel carbapenems to the clinic.

Here we engineer heterologous biosynthesis of the carbapenem antibiotic (5R)-carbapen-2-em-3-carboxylic acid (known as Car) within *E. coli*. Despite our use of low-density shake-flask cultures, we surpass carbapenem titers reported using wild-type *Streptomyces* species cultivated in tank fermenters. As the biosynthetic pathways of all known carbapenems share early intermediates¹⁷, our pathway provides a universal platform that could potentially be further engineered for production of any carbapenem, including novel derivatives generated via in vivo combinatorial biochemistry. We additionally demonstrate how *E. coli* cells can be stabilized against

¹Department of Bionanoscience, Kavli Institute of Nanoscience, Delft University of Technology, Delft, the Netherlands. ²Centre for Research and Interdisciplinarity (CRI), Paris Descartes University, Paris, France. ³Department of Biotechnology, Delft University of Technology, Delft, the Netherlands. *e-mail: G.E.Bokinsky@tudelft.nl

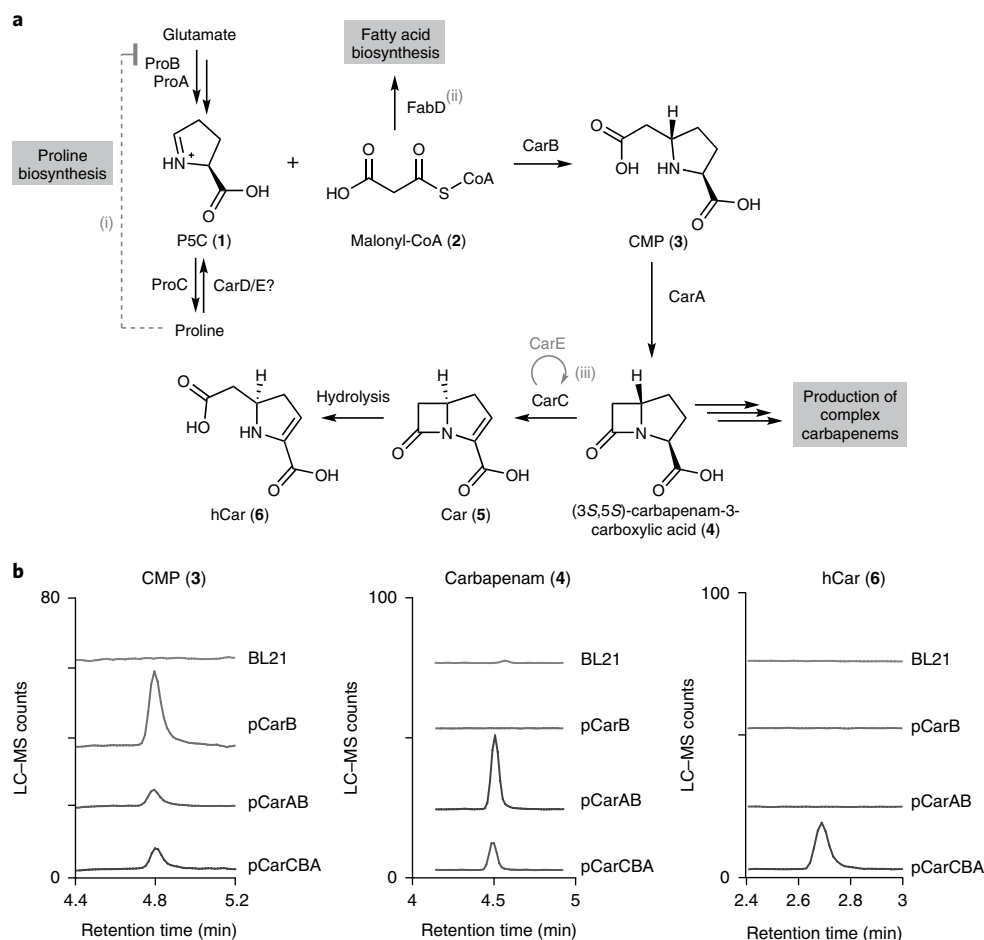


Fig. 1 | The Car biosynthesis pathway and LC-MS detection of synthetic intermediates and products. **a**, The enzyme CarB couples P5C (**1**), an intermediate of proline synthesis, with the fatty acid precursor malonyl-CoA (**2**) to yield (2S,5S)-5-carboxymethylproline (CMP, **3**). CarA catalyzes ATP-dependent cyclization to form the β -lactam ring, generating (3S,5S)-carbapenam-3-carboxylic acid (**4**), the precursor to all known naturally occurring carbapenems. CarC catalyzes two enzymatic steps, C5 epimerization and C2–C3 desaturation, to produce the bioactive carbapenem nucleus of Car (**5**). As with all carbapenems, the β -lactam ring of Car is susceptible to spontaneous hydrolysis, forming hCar (**6**). As indicated, the enzyme CarD and the ferredoxin CarE have been previously proposed to produce **1** from proline. Highlighted are the strategies employed to increase Car production: (i) increasing **1** by relieving allosteric inhibition by proline; (ii) eliminating consumption of **2** by FabD; (iii) regenerating CarC activity by expressing the ferredoxin CarE (our proposed mechanism). **b**, Representative chromatograms of Car pathway metabolites **3**, **4** and byproduct **6** detected in cultures of *E. coli* pCarB, pCarAB, pCarCBA, and BL21. Fragmentation spectra are included in Supplementary Fig. 1.

carbapenem-induced lysis to further increase antibiotic productivity. Such approaches will enable the production of carbapenems from engineered microbes and are likely applicable to heterologous biosynthesis of other bactericidal cell-wall-targeting compounds.

Results

Heterologous production of a carbapenem antibiotic. The antibiotic Car (**5**) is biosynthesized¹⁸ from pyrroline 5-carboxylate (P5C, **1**), an intermediate of proline biosynthesis from glutamate (Fig. 1a), and malonyl-CoA (**2**), a substrate of fatty acid synthesis. A previous study established the enzymes required for Car production by cloning the complete gene cluster from *Pectobacterium carotovorum* in *E. coli*¹⁹; however, titers of Car were not reported. We cloned the codon-optimized minimal Car pathway into a high-copy-number plasmid (pCarCBA) that was transformed into *E. coli* BL21. Car production cultures were grown in MOPS-based minimal medium supplemented with glucose and glutamate.

We developed an LC-MS method to quantify Car pathway metabolites in culture supernatants. As the product **5** is relatively unstable (3h estimated half-life²⁰), we instead quantified hydrolyzed Car (hCar, **6**) as a measure of pathway productivity.

An LC-MS signal from a compound matching the expected 171 m/z ratio of **6** was detected exclusively in cultures expressing the complete pathway (BL21 pCarCBA) under control of an IPTG-inducible promoter P_{lacUV5} (Fig. 1b). Control cultures expressing incomplete Car pathways (BL21 pCarB and BL21 pCarAB) were used to identify LC-MS signals corresponding to the pathway intermediates (2S,5S)-5-carboxymethylproline (CMP, **3**) and (3S,5S)-carbapenam-3-carboxylic acid (**4**) (173 m/z and 155 m/z , respectively). Fragmentation spectra of each compound further supported our assignments (Supplementary Fig. 1).

Metabolic engineering of the Car pathway. Expression of the *carD* and *carE* genes from the *P. carotovorum* Car gene cluster is known to substantially increase Car production^{19,21}. CarD and CarE have sequence similarity with proline dehydrogenase from *Drosophila melanogaster* and [2Fe–2S] ferredoxins, respectively¹⁹, leading to the hypothesis that CarD increases Car production by converting proline into the CarB substrate **1**, with CarE presumably acting as the reducing cofactor for CarD¹⁷ (Fig. 1a). We co-expressed both *carD* and *carE* with *carCBA* (BL21 pCarCBADE) and observed an 11-fold increase in Car productivity (defined as concentrations of **6** per unit

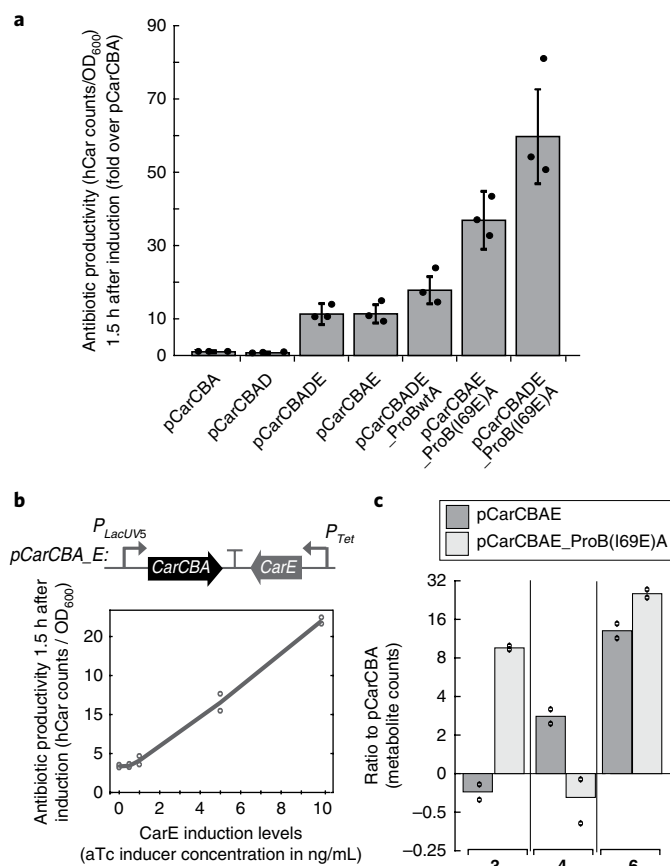


Fig. 2 | Metabolic engineering of the Car biosynthesis pathway in *E. coli*. **a**, Successive metabolic engineering steps increased productivity by 60-fold over the minimal pathway (pCarCBA). Productivity is calculated from LC-MS counts of **6** in culture supernatants divided by the cell density (OD₆₀₀) 1.5 h after induction. Each bar represents the mean \pm s.d. of three independent 5-mL cell cultures grown separately from a common culture. **b**, Top, schematic of plasmid pCarCBA_E encoding CarCBA and CarE controlled by orthogonal promoters P_{LacUV5} (IPTG-inducible) and P_{Tet} (aTc-inducible), respectively. Bottom, effect of varying concentrations of aTc (CarE induction) on **6** productivity (**6** counts/OD₆₀₀) recorded 1.5 h after induction. Solid line represents mean productivity of two biological replicates measured at each aTc concentration. **c**, Mean ratios (normalized by LC-MS counts of BL21 pCarCBA) of pathway metabolites observed 2 h after induction of two 25-mL cultures. For all graphs, dots report values from individual replicates.

biomass per unit time; Fig. 2a) compared to the minimal pathway pCarCBA. To further investigate the specific roles of CarD and CarE, we co-expressed each protein individually with CarCBA. Although CarD did not significantly increase Car productivity when expressed without CarE, expression of CarE alone recovered the 11-fold productivity increase observed with CarDE expression (Fig. 2a).

We next separated expression of *carE* from *carCBA* by cloning it into a separate operon controlled by an orthogonal promoter (P_{Tet} , strain BL21 pCarCBA_E) and titrated induction of CarE while maintaining constant induction of CarCBA. Car productivity correlated with increasing induction of CarE (Fig. 2b). The presence of the predicted [2Fe–2S] cluster of CarE was confirmed using whole-cell EPR spectroscopy^{22,23}. An in vivo EPR spectrum obtained from *E. coli* BL21 overexpressing CarE displayed a clear [2Fe–2S] cluster signal that is absent in whole-cell EPR spectra of wild-type *E. coli* BL21 (Supplementary Fig. 2a). The observed *g*-values (2.04; 1.95; 1.89) closely correlate with the known [2Fe–2S] cluster signal of the

spinach ferredoxin protein (2.05; 1.96; 1.89)²⁴. Mutations of cysteine residues (C43S and C46S) that form the FeS cluster suppressed the [2Fe–2S] signal (Supplementary Fig. 2b) and eliminated the high-production phenotype (Supplementary Fig. 3a), indicating that the FeS cluster is required to increase Car production. We next tested whether CarE facilitates production of **1** by quantifying **3**, the product of CarB. Co-expression of *carD* with *carB* (strain BL21 pCarBD) increased production of **3** by approximately 70%, consistent with the hypothesized assignment of CarD as a proline dehydrogenase. However, the CarD-dependent increase in **3** does not require CarE, and co-expression of *carE* with *carB* (strain BL21 pCarBE) did not increase production of **3** compared to BL21 pCarB (Supplementary Fig. 3b). Finally, a BLAST search²⁵ failed to detect a CarD homolog in the *E. coli* genome that may interact with CarE. We thus conclude that CarE does not influence any catalytic step upstream of CarA.

If CarE does not facilitate CarD activity, what could be the role of a ferredoxin in the Car pathway? CarE is unlikely to facilitate the synthesis of **4** from **3** by CarA, as this reaction has been characterized and is not known to require reducing equivalents²⁶. Car production is severely limited by the activity of CarC, a redox-active Fe(II)- and 2-ketoglutarate-dependent enzyme, which catalyzes both C5 stereoinversion and C2–C3 desaturation of **4** to yield **5** (ref. 27). A recent mechanism based upon extensive in vitro evidence proposed that stereoinversion by CarC is limited to a single turnover, as the reaction oxidizes the bound Fe(II) to Fe(III)²⁸. Regeneration of Fe(II) by a reducing cofactor is thus required for subsequent C2–C3 desaturation and further stereoinversions. On the basis of our results, and the location of the *carE* gene within the native *car* operon, we propose that CarE may be the primary reducing cofactor of CarC. CarE overexpression likely increases Car productivity by accelerating CarC reduction after stereoinversion. Further in vitro studies using purified CarC and CarE are needed to evaluate this hypothesis.

To further improve Car productivity, we sought to increase the abundance of the CMP precursor **1**, an intermediate of the proline biosynthesis pathway. In *E. coli*, **1** is generated from glutamate by the enzymes ProB (glutamate 5-kinase) and ProA (glutamate 5-semialdehyde dehydrogenase). As with other amino acid biosynthetic pathways, proline inhibits its own synthesis via feedback inhibition of ProB²⁹ (Fig. 1a). Production of **3**, and ultimately carbapenems, may therefore be limited by low concentrations of **1**. We co-expressed the Car pathway with ProA and feedback-resistant mutants of ProB²⁹ (Supplementary Fig. 4). Expression of the mutant ProB I69E (BL21 pCarCBAE_ProB(I69E)A and BL21 pCarCBADE_ProB(I69E)A) further improved productivity of **6** by three-fold (Fig. 2a). In contrast, expression of wild-type (proline-inhibited) ProB and ProA resulted in a smaller productivity increase (Fig. 2a) and did not increase titers of **3** (Supplementary Fig. 5).

Co-expressing CarE and feedback-resistant ProBA improved productivity of **5** shortly after induction by nearly 60-fold compared to the minimal pathway (Fig. 2a). We quantified biosynthesis intermediates **3** and **4** to identify bottlenecks in our engineered pathway that may limit production of **5**. Figure 2c depicts concentrations of **3**, **4** and **6** 2 h after induction in 25-mL cultures. As expected, expression of CarE appears to increase flux through the Car pathway by conversion of **4**, whereas expression of feedback-resistant ProB and ProA improved production of **3** by at least 13-fold compared to BL21 pCarCBAE, likely by increasing concentrations of precursor **1**. The accumulation of **3** in strains expressing feedback-resistant ProB(I69E) and ProA suggests that insufficient CarA activity acts as a bottleneck in our engineered pathway and indicates that this enzyme could be a target for future protein engineering.

Improved antibiotic productivity triggers cell lysis. Production of antibiotics in susceptible cells is expected to limit achievable titers by inhibiting biomass production (growth). In particular, production of β -lactam antibiotics, which target cell-wall synthesis,

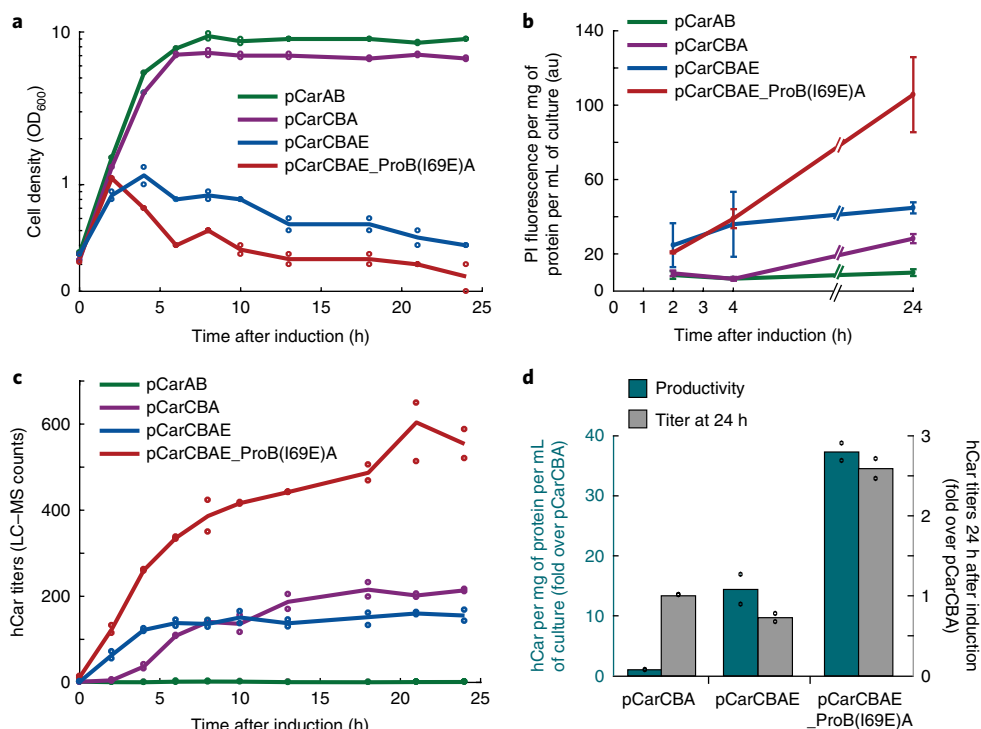


Fig. 3 | Car production causes lysis and limits achievable titers. **a**, Growth curves of engineered strains after induction of the Car pathway. **b**, Cell permeability measurements in Car-producing cultures after induction. Each line represents the mean \pm s.d. of three biological replicates. **c**, LC-MS quantification of **6** after induction. Solid lines depict the mean of two biological replicates. **d**, Comparison of productivity of **6** 2 h after induction with titers of **6** achieved at 24 h (normalized to values obtained for BL21 pCarCBA). Productivity of lysed cultures was estimated by titers of **6** per total protein extracted in culture samples collected 2 h after induction (green bars). Bars represent the mean of two biological replicates. For all graphs, dots report values from individual replicates.

should further limit titers by triggering lysis and arresting biosynthesis. Measurements of optical density at 600 nm (OD_{600}) clearly indicated that growth inhibition occurred very early (2 h) after induction of high-performing pathways (Fig. 3a). Growth inhibition reduced maximum biomass achievable (as estimated by OD_{600}) by nine-fold compared to a control strain (BL21 pCarAB). Car-producing cultures accumulated cell debris characteristic of cell lysis, which was also reflected by decreasing trends in OD_{600} that were apparent 3–5 h after induction (Fig. 3a). Measurements of membrane permeability using propidium iodide (PI) confirmed that permeability increases early after induction of the Car pathway and correlates with Car productivity, consistent with Car-induced lysis (Fig. 3b). Measurements of cell viability, as determined from counts of colony forming units (CFU) 24 h after induction, confirmed that cell death correlates with productivity (Supplementary Fig. 6).

Growth inhibition by **5** prevented the translation of productivity improvements into titer increases. Twenty-five-milliliter cultures of BL21 pCarCBAE exhibited 14-fold higher productivity than BL21 pCarCBA shortly after the pathway was induced but reached only 70% of the titer of **6** measured at 24 h. BL21 pCarCBAE_ProB(I69E)A (37-fold higher productivity) improved 24-h titers of **6** by only 2.6-fold (Fig. 3c,d). This was partly caused by the considerable reduction in biomass produced caused by growth inhibition and lysis by **5**. Production of **5** by cultures of BL21 pCarCBAE_ProB(I69E)A apparently continued during lysis, but at a decreasing rate, likely owing to arrest of cell metabolism (Fig. 3a,c).

Increased antibiotic tolerance improves Car production. The toxicity of Car limits the achievable cell density of production cultures, which in turn severely limits antibiotic titers. We sought to engineer

strains and fermentations to improve tolerance to **5** without compromising productivity. A straightforward approach to mitigate biomass limitation caused by Car toxicity is simply to delay expression of the Car pathway until late exponential growth, when a sufficient amount of biomass has been produced. Induction of BL21 pCarCBAE_ProB(I69E)A at a higher cell density ($OD_{600}=1$ rather than $OD_{600}=0.4$) increased both maximum biomass and **6** titer by nearly two-fold (Supplementary Fig. 7a). However, lysis was still observed in late-induced cultures as an OD_{600} decrease between 3 and 24 h (Supplementary Fig. 7b).

To prevent lysis of Car-producing cells and extend Car production further, we explored natural mechanisms that confer tolerance to β -lactams. A phenotype known as persistence, in which cells are temporarily immune to antibiotic exposure, can be artificially induced by expression of growth-arresting toxin proteins³⁰. Overexpression of the toxin HipA causes growth arrest and confers β -lactam tolerance by triggering guanosine tetraphosphate synthesis (ppGpp)³¹, which directly inhibits the phospholipid synthesis enzyme PlsB³². HipA-arrested cultures survive β -lactam exposure while remaining metabolically active and are able to sustain production of the isoprenoid precursor mevalonate from a heterologous pathway for several days while resisting phage-induced lysis³¹. We tested whether growth arrest by HipA could also prevent Car-induced lysis. Although HipA-arrested cultures sustained production of **5** and exhibited lower cell permeability (Supplementary Fig. 8a,d), higher titers were not achieved, likely because of decreased production of **3** (Supplementary Fig. 8c).

We were, however, encouraged by the improved tolerance of HipA-arrested cells against Car-induced lysis. β -lactam tolerance can also be achieved by direct inhibition of fatty acid synthesis (FAS) even without ppGpp accumulation³³. Inhibition of FAS using the

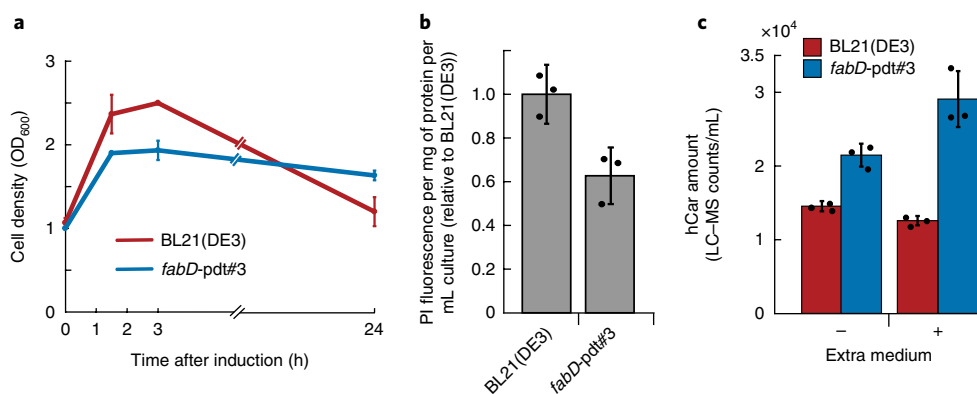


Fig. 4 | Inhibition of fatty acid synthesis increases antibiotic tolerance and Car pathway flux. **a**, Growth curves of BL21(DE3) pCarCBAE_ProB(I69E)A after induction, indicating lysis (45% OD₆₀₀ decrease) in BL21(DE3), which is reduced in the *fabD-pdt#3 pmf*-Lon strain (19% OD₆₀₀ decrease). Protease-driven depletion of FabD in the strain *fabD-pdt#3 pmf*-Lon was simultaneously induced with Car production. **b**, Cell permeability measurements 24 h after induction, indicating decreased lysis in *fabD-pdt#3* strains. **c**, Total Car produced (**6** titer multiplied by culture volume) 24 h after induction. Cultures supplemented with 25 mL fresh production medium 1.5 h after induction are indicated with a plus sign. Solid lines and bars represent the mean \pm s.d. of three biological replicates. For all graphs, dots report values from individual replicates.

mycotoxin cerulenin, an inhibitor of FabF and FabB enzymes, starves phospholipid synthesis and confers β -lactam tolerance³³. Furthermore, by inhibiting fatty acid elongation, cerulenin causes accumulation of **2** (ref.³⁴), a substrate of CarB. Inhibition of FAS by cerulenin could thus improve carbapenem production by *E. coli* via two mechanisms: by decreasing lysis and by increasing availability of a precursor metabolite^{35,36}. Treatment of Car-producing cultures with 20 μ g/mL cerulenin indeed decreased cell permeability and Car-induced lysis (Supplementary Fig. 8a,b). Fluorescence readings from a genetic sensor³⁷ confirmed that cerulenin treatment increased accumulation of **2** (Supplementary Fig. 9a). Addition of cerulenin increased titers of **3** by nearly five-fold (Supplementary Fig. 8c). Although accumulation of **2** did not significantly improve titer of **6** under these experimental conditions (Supplementary Fig. 8d), observed increases in **3** confirmed that FAS inhibition improves flux into the Car pathway while alleviating Car-induced lysis. We thus decided to further optimize FAS inhibition to improve Car production.

As the cost of cerulenin makes its use in large-scale fermentations impractical, we sought a genetically encoded trigger for FAS inhibition. We used a recently developed synthetic protein-degradation system to eliminate FAS enzymes that consume **2** (ref.³⁸). The *mf*-Lon protease degrades proteins carrying a specific C-terminal tag (pdt). We thus appended a tag that confers a fast degradation rate (pdt#3)³⁸ to chromosomally encoded fatty acid synthesis enzymes (FabB, FabF and FabD) and induced expression of the *mf*-Lon protease. Similarly to cerulenin treatment, induction of the *mf*-Lon protease arrested growth while leading to accumulation of **2** in BL21 *fabD-pdt#3* (Fig. 4a; Supplementary Fig. 9) and increased production of **3** in BL21 *fabD-pdt#3* pCarCBAE_ProB(I69E)A (Supplementary Fig. 10). Induction of FabD degradation reduced both cell lysis and membrane permeability of Car-producing cells, indicating that FAS inhibition via FabD degradation decreases Car toxicity (Fig. 4a,b). Furthermore, FabD degradation increased Car production (normalized to culture volume) by 50% (Fig. 4c). Inhibition of FAS by FabD degradation also decreased apparent lysis caused by the complex carbapenem antibiotic imipenem (Supplementary Fig. 11).

To confirm that better tolerance can directly lead to improved Car titers, we tested the stability of Car production in FAS-inhibited cells by supplementing cultures with fresh medium. We hypothesized that addition of fresh medium would prolong productivity of metabolically active cultures, either by restoring depleted nutrients or by diluting inhibitory waste products.

No additional **5** was produced in control cultures after medium supplementation, suggesting that the cultures had been metabolically inactivated by lysis. However, biosynthetic activity continued in FAS-inhibited cultures, and the total amount of **6** increased by 40% (Fig. 4c). Overall, Car production in FAS-arrested cultures supplemented with fresh medium improved by two-fold compared to control cultures. We attribute this increase to a combination of antibiotic tolerance and increased concentrations of **2** available for synthesis of **3** by CarB.

Estimating Car titers to benchmark strain performance. As authentic chemical standards for **5** and **6** are not available, estimating Car titers via LC-MS alone is not possible. Therefore, we used differential UV spectroscopy, a technique used to quantify carbapenems in both crude fermentation broths and purified extracts^{16,39,40}. Carbapenems exhibit UV absorption that is lost upon aminolysis of the chromophore by hydroxylamine⁴¹. Thus, carbapenem concentrations can be calculated by measuring the UV absorbance eliminated after hydroxylamine treatment. We confirmed the reliability of differential spectroscopy using an imipenem standard added to lysed *E. coli* cultures (Supplementary Fig. 12; Supplementary Table 1a). Next, we used differential spectroscopy to quantify **5** in cultures of BL21 pCarBAE_ProB(I69E)A 3 h after induction, which is when we estimate that most **5** has not yet been hydrolyzed. Using the extinction coefficient previously determined for Car⁴², we calculated a titer of 5 of 17.0 ± 5.1 mg/L (Supplementary Fig. 13; Supplementary Table 1a).

We sought to determine the total amount of **5** produced over a 24-h fermentation to enable comparisons with native carbapenem-producing species. However, the near-total hydrolysis of **5** after 24 h precludes the direct use of differential spectroscopy (Supplementary Fig. 13). Therefore, we estimated total **5** produced over 24 h by multiplying the 3-h titer of **5** with the ratio of LC-MS counts of **6** at 3 h and 24 h after induction. In the absence of FAS arrest, BL21(DE3) pCarBAE_ProB(I69E)A produced 37.3 ± 16.7 mg/L of **5**, whereas FAS-arrested cells produced 54.1 ± 17.4 mg/L (detailed calculations are in Supplementary Table 1b). These titers demonstrate a substantial improvement over carbapenem titers achieved by *S. cattleya*.

Discussion

Our results demonstrate how *E. coli* can be harnessed as a heterogeneous platform for biosynthesis of bactericidal antibiotics. The genetic tractability and fast growth of *E. coli* enabled rational

engineering and short fermentation times: in less than 24 h, and despite low cell density, titers of **6** reached 54.1 ± 17.4 mg/L, whereas tank fermentation cultures of wild-type *S. cattleya* require at least 5 d to reach a final thienamycin titer of 4 mg/L¹⁶. Although **5** is too unstable to be clinically useful, our pathway modifications, which increase flux to the universal carbapenem precursors **3** and **4**, could be used to improve production of more stable carbapenem antibiotics, either in *E. coli* or in a carbapenem-producing *Streptomyces* host. The co-expression of carbapenem tailoring enzymes, obtained either from the variety of known carbapenem pathways or via modification of existing enzymes¹¹, could generate novel derivatives and further expand carbapenem diversity¹⁸.

Increasing the concentrations of carbapenem precursors **1** and **2** improved productivity, indicating that the activity of CarB, and thus flux through the carbapenem pathway, is limited by precursor availability. Increasing precursor concentrations has been shown repeatedly to improve biosynthesis of other antibiotic families^{43,44}, which is consistent with findings that flux through microbial biosynthetic pathways are often limited by precursor metabolites⁴⁵. We have also identified a likely reducing partner for the enzyme CarC, an unusual enzyme with dual activities that is notorious for its low catalytic rates. Overexpression of CarE increased Car productivity by 11-fold, illustrating the importance of identifying and overexpressing reducing partners for redox enzymes in biosynthetic pathways.

The identification of additional reducing partners will likely prove necessary for heterologous expression of complex carbapenem pathways, which include several redox-active iron-sulfur (FeS) enzymes⁴⁶. The requirement of FeS enzymes for complex carbapenem biosynthesis presents a barrier to heterologous carbapenem production in yeast, which are otherwise well-suited for producing β -lactam antibiotics because of their natural tolerance⁹. Engineering functional expression of bacterial FeS enzymes in eukaryotes has proved challenging because of apparent incompatibilities of bacterial FeS enzymes with eukaryotic FeS assembly pathways⁴⁷. Until FeS enzymes can be reliably transferred between prokaryotes and eukaryotes, bacterial species may be more amenable hosts for heterologous carbapenem production.

Our approach for mitigating Car toxicity provides a strategy for producing growth-inhibiting compounds within susceptible hosts. Delaying induction of Car biosynthesis to allow biomass accumulation improved Car titer. Timed arrest of FAS synthesis, which confers tolerance against β -lactam antibiotics, prolonged Car production and improved titers further. As FAS arrest protects cells against β -lactam antibiotics, including complex carbapenems such as imipenem⁴⁸, this approach will likely prove effective for production of clinically relevant carbapenems. The use of fed-batch cultivation to reach high cell densities (i.e., 20-fold more than the densities achieved here), together with timed FAS arrest and continued nutrient feeding, may bring carbapenem titers close to industrially relevant levels. The use of self-inducing promoters⁴⁹ to trigger antibiotic production and FAS arrest would remove the dependence of the present system on chemical inducers, which are not economical at large scales. Other methods for improving tolerance, such as mutating the cellular target of carbapenem, or expressing efflux channels, could further translate productivity improvements into increased titers. Combined with our engineered carbapenem pathway, such approaches could fully capitalize on the strengths of *E. coli* as a production host and bring natural and novel carbapenems closer to clinical use.

Methods

Methods, including statements of data availability and any associated accession codes and references, are available at <https://doi.org/10.1038/s41589-018-0084-6>.

Received: 30 November 2017; Accepted: 27 April 2018;
Published online: 25 June 2018

References

- Gillespie, D. E. et al. Isolation of antibiotics turbomycin a and B from a metagenomic library of soil microbial DNA. *Appl. Environ. Microbiol.* **68**, 4301–4306 (2002).
- Ling, L. L. et al. A new antibiotic kills pathogens without detectable resistance. *Nature* **517**, 455–459 (2015).
- Rutledge, P. J. & Challis, G. L. Discovery of microbial natural products by activation of silent biosynthetic gene clusters. *Nat. Rev. Microbiol.* **13**, 509–523 (2015).
- Brady, S. F., Simmons, L., Kim, J. H. & Schmidt, E. W. Metagenomic approaches to natural products from free-living and symbiotic organisms. *Nat. Prod. Rep.* **26**, 1488–1503 (2009).
- Olano, C., Lombó, F., Méndez, C. & Salas, J. A. Improving production of bioactive secondary metabolites in actinomycetes by metabolic engineering. *Metab. Eng.* **10**, 281–292 (2008).
- Katz, L. & Khosla, C. Antibiotic production from the ground up. *Nat. Biotechnol.* **25**, 428–429 (2007).
- Demain, A. L. From natural products discovery to commercialization: a success story. *J. Ind. Microbiol. Biotechnol.* **33**, 486–495 (2006).
- Medema, M. H., Breitling, R., Bovenberg, R. & Takano, E. Exploiting plug-and-play synthetic biology for drug discovery and production in microorganisms. *Nat. Rev. Microbiol.* **9**, 131–137 (2011).
- Awan, A. R. et al. Biosynthesis of the antibiotic nonribosomal peptide penicillin in baker's yeast. *Nat. Commun.* **8**, 15202 (2017).
- Freeman, M. F., Vagstad, A. L. & Piel, J. Polytheonamide biosynthesis showcasing the metabolic potential of sponge-associated uncultivated 'Entotheonella' bacteria. *Curr. Opin. Chem. Biol.* **31**, 8–14 (2016).
- Hamed, R. B., Henry, L., Claridge, T. D. W. & Schofield, C. J. Stereoselective production of dimethyl-substituted carbapenams via engineered carbapenem biosynthesis enzymes. *ACS Catal.* **7**, 1279–1285 (2017).
- Zhang, H., Wang, Y., Wu, J., Skalina, K. & Pfeifer, B. A. Complete biosynthesis of erythromycin A and designed analogs using *E. coli* as a heterologous host. *Chem. Biol.* **17**, 1232–1240 (2010).
- McKenna, M. Antibiotic resistance: the last resort. *Nature* **499**, 394–396 (2013).
- Papp-Wallace, K. M., Endimiani, A., Taracila, M. A. & Bonomo, R. A. Carbapenems: past, present, and future. *Antimicrob. Agents Chemother.* **55**, 4943–4960 (2011).
- Wei, W. J., Yang, H. F., Ye, Y. & Li, J. B. Bin. New Delhi metallo-beta-lactamase-mediated carbapenem resistance: Origin, diagnosis, treatment and public health concern. *Chin. Med. J. (Engl.)* **128**, 1969–1976 (2015).
- Kahan, J. S. et al. Thienamycin, a new beta-lactam antibiotic. I. Discovery, taxonomy, isolation and physical properties. *J. Antibiot. (Tokyo)* **32**, 1–12 (1979).
- Hamed, R. B. et al. The enzymes of β -lactam biosynthesis. *Nat. Prod. Rep.* **30**, 21–107 (2013).
- Coulthurst, S. J., Barnard, A. M. L. & Salmond, G. P. C. Regulation and biosynthesis of carbapenem antibiotics in bacteria. *Nat. Rev. Microbiol.* **3**, 295–306 (2005).
- McGowan, S. J. et al. Analysis of bacterial carbapenem antibiotic production genes reveals a novel beta-lactam biosynthesis pathway. *Mol. Microbiol.* **22**, 415–426 (1996).
- Pfaendler, H. R., Gosteli, J., Woodward, R. B. & Rihs, G. Structure, reactivity, and biological activity of strained bicyclic β -lactams. *J. Am. Chem. Soc.* **103**, 4526–4531 (1981).
- McGowan, S. J. et al. Analysis of the carbapenem gene cluster of *Erwinia carotovora*: definition of the antibiotic biosynthetic genes and evidence for a novel β -lactam resistance mechanism. *Mol. Microbiol.* **26**, 545–556 (1997).
- van Vugt-Lussenburg, B. M., van der Weel, L., Hagen, W. R. & Hagedoorn, P. L. Biochemical similarities and differences between the catalytic [4Fe-4S] cluster containing fumarases FumA and FumB from *Escherichia coli*. *PLoS One* **8**, e55549 (2013).
- McHugh, J. P. et al. Global iron-dependent gene regulation in *Escherichia coli*. A new mechanism for iron homeostasis. *J. Biol. Chem.* **278**, 29478–29486 (2003).
- Stiefel, E. I. & George, G. N. in *Bioinorganic Chemistry* (eds Bertini, I., Gray, H.B., Lippard, S.J. & Valentine, J.S.) Ch. 7 (University Science Books, Mill Valley, CA, 1994).
- Altschul, S. F., Gish, W., Miller, W., Myers, E. W. & Lipman, D. J. Basic local alignment search tool. *J. Mol. Biol.* **215**, 403–410 (1990).
- Gerratana, B., Stapon, A. & Townsend, C. A. Inhibition and alternate substrate studies on the mechanism of carbapenem synthetase from *Erwinia carotovora*. *Biochemistry* **42**, 7836–7847 (2003).
- Stapon, A., Li, R. & Townsend, C. A. Carbapenem biosynthesis: confirmation of stereochemical assignments and the role of CarC in the ring stereoinversion process from L-proline. *J. Am. Chem. Soc.* **125**, 8486–8493 (2003).
- Chang, W. C. et al. Mechanism of the C5 stereoinversion reaction in the biosynthesis of carbapenem antibiotics. *Science* **343**, 1140–1144 (2014).

29. Pérez-Arellano, I., Carmona-Álvarez, F., Gallego, J. & Cervera, J. Molecular mechanisms modulating glutamate kinase activity. Identification of the proline feedback inhibitor binding site. *J. Mol. Biol.* **404**, 890–901 (2010).
30. Korch, S. B. & Hill, T. M. Ectopic overexpression of wild-type and mutant *hipA* genes in *Escherichia coli*: effects on macromolecular synthesis and persister formation. *J. Bacteriol.* **188**, 3826–3836 (2006).
31. Bokinsky, G. et al. HipA-triggered growth arrest and β -lactam tolerance in *Escherichia coli* are mediated by RelA-dependent ppGpp synthesis. *J. Bacteriol.* **195**, 3173–3182 (2013).
32. Heath, R. J., Jackowski, S. & Rock, C. O. Guanosine tetraphosphate inhibition of fatty acid and phospholipid synthesis in *Escherichia coli* is relieved by overexpression of glycerol-3-phosphate acyltransferase (plsB). *J. Biol. Chem.* **269**, 26584–26590 (1994).
33. Rodionov, D. G. & Ishiguro, E. E. Dependence of peptidoglycan metabolism on phospholipid synthesis during growth of *Escherichia coli*. *Microbiology* **142**, 2871–2877 (1996).
34. Omura, S. The antibiotic cerulenin, a novel tool for biochemistry as an inhibitor of fatty acid synthesis. *Bacteriol. Rev.* **40**, 681–697 (1976).
35. Rogers, J. K. & Church, G. M. Genetically encoded sensors enable real-time observation of metabolite production. *Proc. Natl Acad. Sci. USA* **113**, 2388–2393 (2016).
36. Yang, Y., Lin, Y., Li, L., Linhardt, R. J. & Yan, Y. Regulating malonyl-CoA metabolism via synthetic antisense RNAs for enhanced biosynthesis of natural products. *Metab. Eng.* **29**, 217–226 (2015).
37. Fehér, T., Libis, V., Carbonell, P. & Faulon, J.-L. A sense of balance: experimental investigation and modeling of a malonyl-CoA sensor in *Escherichia coli*. *Front. Bioeng. Biotechnol.* **3**, 46 (2015).
38. Cameron, D. E. & Collins, J. J. Tunable protein degradation in bacteria. *Nat. Biotechnol.* **32**, 1276–1281 (2014).
39. Rosi, D. et al. Mutants of *Streptomyces cattleya* producing N-acetyl and deshydroxy carbapenems related to thienamycin. *J. Antibiot. (Tokyo)* **34**, 341–343 (1981).
40. Wilson, K. E., Kempf, A. J., Liesch, J. M. & Arison, B. H. Northienamycin and 8-epi-thienamycin, new carbapenems from *Streptomyces cattleya*. *J. Antibiot. (Tokyo)* **36**, 1109–1117 (1983).
41. Wagman, G. H. & Cooper, R. *Natural Products Isolation: Separation Methods for Antimicrobials, Antivirals and Enzyme Inhibitors* (Elsevier Science, New York, 1988).
42. Bateson, J. H., Baxter, A. J. G., Roberts, P. M., Smale, T. C. & South-Gate, R. Olivanic acid analogues. Part 1. Total synthesis of the 7-oxo-1-azabicyclo[3.2.0]hept-2-ene-2-carboxylate system and some related β -lactams. *J. Chem. Soc. Perkin Trans. I* **1981**, 3242–3249 (1981).
43. Zabala, D., Braña, A. F., Flórez, A. B., Salas, J. A. & Méndez, C. Engineering precursor metabolite pools for increasing production of antitumor mithramycins in *Streptomyces argillaceus*. *Metab. Eng.* **20**, 187–197 (2013).
44. Gómez, C. et al. Amino acid precursor supply in the biosynthesis of the RNA polymerase inhibitor streptolydigin by *Streptomyces lydicus*. *J. Bacteriol.* **193**, 4214–4223 (2011).
45. Zhang, M. M., Wang, Y., Ang, E. L. & Zhao, H. Engineering microbial hosts for production of bacterial natural products. *Nat. Prod. Rep.* **33**, 963–987 (2016).
46. Marous, D. R. et al. Consecutive radical S-adenosylmethionine methylations form the ethyl side chain in thienamycin biosynthesis. *Proc. Natl Acad. Sci. USA* **112**, 10354–10358 (2015).
47. Kirby, J. et al. Engineering a functional 1-deoxy-d-xylulose 5-phosphate (DXP) pathway in *Saccharomyces cerevisiae*. *Metab. Eng.* **38**, 494–503 (2016).
48. Tuomanen, E. Phenotypic tolerance: the search for β -lactam antibiotics that kill nongrowing bacteria. *Rev. Infect. Dis.* **8** (Suppl. 3), S279–S291 (1986).
49. Briand, L. et al. A self-inducible heterologous protein expression system in *Escherichia coli*. *Sci. Rep.* **6**, 33037 (2016).

Acknowledgements

We thank D.E. Cameron and J.J. Collins (Massachusetts Institute of Technology) for the gift of strains for designing tunable protein degradation. We are grateful to V. Libis (Rockefeller University) for the gift of the plasmid pCFR. We thank F. Wu for valuable scientific discussions throughout the project and B. Beaumont for helpful comments with the manuscript. This work was supported by startup funds provided to G.B. from TU Delft and the Department of Bionanoscience, as well as the Netherlands Organization for Scientific Research (NWO/OCW), as part of the Frontiers of Nanoscience program. P.-L.H. was supported by grant NWO–CW 711.014.006 from the Council for Chemical Sciences of the NWO.

Author contributions

G.B. and H.S. designed the experiments. H.S. performed the experiments and analyzed the results. S.G. constructed strains and performed experiments for studying the function of CarE. H.T.M. performed preliminary experiments to study FAS inhibition. P.-L.H. conducted EPR spectroscopy and analyzed related data. H.S. and N.v.d.B. developed LC–MS methods, with early assistance from M.J.N. G.B. supervised the research. H.S. and G.B. wrote the manuscript.

Competing interests

G.B. and H.S. have filed a patent application covering metabolic engineering of carbapenem pathways.

Additional information

Supplementary information is available for this paper at <https://doi.org/10.1038/s41589-018-0084-6>.

Reprints and permissions information is available at www.nature.com/reprints.

Correspondence and requests for materials should be addressed to G.B.

Publisher's note: Springer Nature remains neutral with regard to jurisdictional claims in published maps and institutional affiliations.

Methods

Strains and growth medium. *E. coli* BL21(DE3) was used for Car production experiments. We used cells freshly transformed with plasmids encoding the Car pathway. Transformants were grown overnight on selective LB agar plates at 37 °C, after which plates were stored at 4 °C. Liquid cultures inoculated from colonies bearing the Car pathway showed poor growth if the colonies were kept longer than 48 h. Car production cultures were grown in MOPS-based minimal medium (8.372 g L⁻¹ MOPS, 0.717 g L⁻¹ tricine, 2.92 g L⁻¹ NaCl, 11 mg L⁻¹ MgCl₂•7H₂O, 0.56 μg L⁻¹ CaCl₂, 200 μL micronutrient stock⁵⁰) supplemented with 4 g L⁻¹ D-glucose, 28.5 mM NH₄Cl, 10 μM FeSO₄ and 5 g L⁻¹ potassium glutamate. The antibiotics kanamycin (25 μg/mL), ampicillin (50 μg/mL) and chloramphenicol (17.5 μg/mL) were added when appropriate. All strains and plasmids used in this work are listed in Supplementary Table 2.

Plasmid construction. All plasmids were constructed using Gibson assembly⁵¹ in *E. coli* DH5α. Genes encoding the Car enzymes from *P. carotovorum* (CarABCDE) were codon optimized for expression in *E. coli*. *proB* and *proA* were cloned from *E. coli* BL21(DE3) genomic DNA (primers in Supplementary Table 3). The mutant variants I69E of ProB, and C43S/C46S of CarE were constructed by PCR site-directed mutagenesis using the primers P1 and P2 in Supplementary Table 3. Biosynthetic operons were assembled and cloned into the pBbE5k BglBrick backbone⁵². The plasmid pCarCBA_E was constructed from pCarCBA by addition of the CarE expression unit under control of the inducible P_{Tet} promoter. The reverse sequence of the CarE-inducible expression unit was placed at the 3' end of the bidirectional terminator present on the pBbE5k BglBrick backbone (Fig. 2b). *hipA* was cloned from *E. coli* MG1655 genomic DNA and inserted into the pBbS2c BglBrick backbone to make pHipA (primers in Supplementary Table 3). To construct the *mf*-Lon protease expression vector, we introduced the codon optimized *mf*-Lon gene and strong ribosome binding site from pECL275 (ref. ³⁸) into the pBbA2c⁵² BglBrick backbone. The resulting plasmid *pmf*-Lon contains a chloramphenicol resistance cassette. The derivative plasmid *pmf*-Lon-bis contains an ampicillin resistance cassette instead. All the strains and plasmids constructed in this work are listed in Supplementary Table 2.

Car production protocol. Individual colonies of engineered strains were picked into 5 mL selective production medium and incubated overnight with shaking at 37 °C. From overnight cultures, culture triplicates were seeded at an initial OD₆₀₀ of 0.06 either in 5 mL of selective production medium in culture tubes (small-scale assays) or in 25 mL medium in 250 mL Erlenmeyer flasks (shake-flask assays). Cultures were incubated at 37 °C with shaking (250 r.p.m.). Car production was induced at OD₆₀₀ 0.3–0.45 by addition isopropyl β-D-thiogalactopyranoside (IPTG) to 0.25 mM final concentration. Samples taken from production cultures were cleared by centrifugation, and supernatant aliquots were collected and stored at -80 °C for LC-MS.

CarE titration experiment. As the enzyme CarC is iron dependent, we used an iron-deficient MOPS-based production medium (without FeSO₄ supplementation) to limit Car production from leaky expression of the Car pathway. Individual colonies of BL21(DE3) pCarCBA_E were grown overnight in 5 mL of iron-deficient production medium. Overnight cultures were diluted into 250 mL Erlenmeyer flasks containing 25 mL selective iron-deficient production medium to an initial OD₆₀₀ of 0.06. Cultures were grown at 37 °C with shaking (250 r.p.m.) until reaching an OD₆₀₀ of 0.25. At this point, CarE expression was induced by addition of anhydrotetracycline (aTc). The cultures were further incubated for 2 h, after which CarCBA expression was induced with 0.25 mM IPTG and the medium was supplemented with 10 μM FeSO₄. Cultures were then incubated at 37 °C with shaking, and samples were collected 1.5 h after induction. Supernatant aliquots were collected and stored at -80 °C for LC-MS.

Whole-cell EPR spectroscopy. 25 mL cultures used for EPR spectroscopy were incubated for 2–3 h after induction at 0.3 OD₆₀₀ and cell pellets were recovered by centrifugation. Pellets were stored at -80 °C until analysis. Samples for EPR spectroscopy were prepared by resuspending the pellet in 200 μL sterile 50 mM Tris buffer (pH 8). The suspension was transferred into quartz glass EPR tubes and frozen in liquid nitrogen. X-band EPR measurements were performed using a Bruker ECS-106 EPR spectrometer with a National Instruments interface. Data acquisition was performed using an in-house developed software written in LabVIEW and FORTRAN 90/95. EPR conditions were as follows: microwave frequency, 9.388 GHz; microwave power, 20 mW; modulation frequency, 100 kHz; modulation amplitude, 1.27 mT; temperature, 27 K. EPR spectra were analyzed using programs previously described²³.

Propidium iodide (PI) fluorescence measurements. A stock solution of 10 mM propidium iodide in DMSO was prepared and stored at -20 °C. 100 μL of culture sample was mixed with an equal amount of a 2× PI working solution (prepared by adding 3 μL of stock solution to 1 mL of water). Mixtures were incubated in transparent 96-well plates at room temperature (20–21 °C) in the dark. After 15 min incubation, PI fluorescence was measured using a BioTek Synergy HTX microplate reader, equipped with an excitation filter of 485/20 nm and an emission filter of 620/15 nm with a gain setting of 40.

Total protein quantification in production cultures. Due to Car-induced cell lysis, optical density measurements > 2 h after induction no longer accurately measure total biomass accumulation. We therefore estimated biomass accumulation by measuring the total amount of protein present per volume of culture by chloroform-methanol protein precipitation. We added 400 μL of methanol, 100 μL of chloroform and 300 μL of water to 100 μL of culture. Mixtures were vortexed vigorously and centrifuged at 10,000g for 1 min. The upper MeOH/water layer was carefully removed without disturbing the interface, after which 300 μL of methanol were added to the remaining phase. Mixtures were then vortexed vigorously and centrifuged at 10,000g for 1 min. The supernatant was discarded and pellets obtained were dried by vacuum centrifuge. Protein pellets were resuspended in 10–100 μL binding buffer (6 M urea, pH 7.2). The colorimetric Bradford assay⁵⁴ was used to measure protein concentrations.

Construction of strains with tunable protein degradation. The degradation tag pdt#3 was fused to the C terminus of the genes of interest in *E. coli* BL21(DE3) chromosomal DNA³⁸. For each targeted gene (*fabB*, *fabD* and *fabF*), we generated PCR products that contained the pdt#3 tag amplified from pECT3 and 37–42 bp 5' extensions with homology to the C terminus, and 3' extensions with homology to the immediate 3' untranslated region of the gene of interest. The P1 and P2 primer sequences and full-length primers used to target *fabB*, *fabD* and *fabF* are found in Supplementary Table 3. Genomic pdt#3 insertions were performed using homologous recombination⁵⁵ by transforming the PCR products into *E. coli* BL21(DE3) containing pKD46. Successful insertions were verified by PCR. The kanamycin resistance cassette was subsequently removed using the plasmid pCP20. The resulting strains, *fabB*-pdt#3, *fabD*-pdt#3 and *fabF*-pdt#3, were screened by PCR and verified by DNA sequencing.

Relative malonyl-CoA quantification. We used the transcription-factor-based biosensor plasmid pCFR³⁷, which expresses red fluorescent protein (RFP) in response to intracellular malonyl-CoA. Strains transformed with pCFR were grown to OD₆₀₀ 0.1, and 100 μL culture aliquots were placed on transparent 96-well plates in triplicate. RFP and OD₆₀₀ were monitored using a BioTek Synergy HTX microplate reader, equipped with an excitation filter of 485/20 nm and an emission filter of 620/15 nm with a gain setting of 40.

LC-MS analysis. Metabolite levels in culture supernatants were measured using LC-MS. As 5 is known to rapidly hydrolyze in acid (pH < 3)⁵⁶, all samples were acidified before analysis to hydrolyze any remaining 5 into 6. For each collected sample, 5 μL of supernatant was added to 195 μL ACN with 0.1% formic acid. The mixtures were vortexed, centrifuged at 15,000g for 2 min and incubated for 1 h prior analysis. 2 μL of the sample was injected onto an Agilent ZORBAX HILIC Plus column (100-mm length, 2.1-mm internal diameter, 3.5 μm particle size). Liquid chromatography separation was conducted at 30 °C using a LC-MS system (Agilent) consisting of a binary pump (G1312B), an autosampler (G7167A), a temperature-controlled column compartment (G1316A) and a triple quadrupole mass spectrometer (G6460C) equipped with a standard ESI source. The mobile phase was composed of 25 mM ammonium formate (solvent A) and 100% acetonitrile (solvent B). Samples were separated with a gradient from 95% to 60% of solvent B for 5 min at a flow rate of 0.5 mL/min, which was followed by a gradient from 60% to 50% for 2 min at a flow rate of 0.5 mL/min to 0.6 mL/min and 50% to 95% solvent B for 2 min at 0.7 mL/min, and then held at 95% solvent B for 2 min at a flow of 0.5 mL/min. Peaks were analyzed by MS using ESI ionization in MRM mode. The precursor ion analyzed for each compound (3, 4 and 6) was determined by mass calculation based on their chemical formula. For each compound, fragmentation spectra and MRM settings are found in Supplementary Table 4.

Estimating Car titers. Car concentration is estimated from the difference in absorbance (262 nm) between hydroxylamine-treated and untreated samples using a molar extinction coefficient previously determined for Car⁴² (4,500) and a pathlength of 0.1 cm. Absorbance was measured using the pedestal mode of a NanoDrop 2000 spectrophotometer. For hydroxylamine treatment, 100 μL of culture supernatants were mixed with hydroxylamine (10 mM final concentration; hydroxylamine solution freshly prepared from NH₂OH HCl, pH 7) in 10 mM KH₂PO₄ pH 7 for 1 h at room temperature. Addition of hydroxylamine did not affect the absorbance spectra of supernatants taken from fosfomicin-lysed cultures that do not produce Car (BL21 pCarAB_ProB(I69E)A, Supplementary Fig. 12a). We validated the use of differential UV spectroscopy by quantifying known concentrations of imipenem added to cultures in order to closely mimic the conditions of Car sampling. Imipenem absorbance (300 nm) was extinguished by hydroxylamine (Supplementary Fig. 12b, c). Calculated values linearly corresponded to known concentrations of imipenem added, with 14% average error at concentrations of 2 mg/L or higher (Supplementary Fig. 12d and detailed calculations in Supplementary Table 1a). For quantification of Car, overnight cultures from individual colonies of BL21 pCarCBAE_ProB(I69E)A were used to inoculate 25 mL production medium at a starting OD₆₀₀ of 0.06 and incubated at 37 °C with shaking (250 r.p.m.) in 250-mL Erlenmeyer flasks. Cultures were induced at OD₆₀₀ 1.0 with 0.25 mM IPTG. 1 mL culture supernatant aliquots were collected 3 h (or 24 h) after induction and cleared by centrifugation.

UV absorption spectra and detailed calculations are described in Supplementary Fig. 13a and Supplementary Table 1. Consistent with the known instability of Car, no hydroxylamine-labile absorbance was detected in samples collected 24 h after induction of Car biosynthesis (Supplementary Fig. 13b).

Statistics. Unless otherwise noted in the figure legend, bars and lines depict averages of independent cell cultures grown from independent bacterial colonies, by which we define biological replicates. Sample sizes are described in the figure legends. Error bars represent ± 1 s.d. from the mean. Dots in figures report values obtained from independent biological replicates.

Reporting Summary. Further information on experimental design is available in the Nature Research Reporting Summary linked to this article.

Data availability. The data that support the findings of this study are available from the corresponding author upon reasonable request.

References

50. Neidhardt, F. C., Bloch, P. L. & Smith, D. F. Culture medium for enterobacteria. *J. Bacteriol.* **119**, 736–747 (1974).
51. Gibson, D. G. et al. Enzymatic assembly of DNA molecules up to several hundred kilobases. *Nat. Methods* **6**, 343–345 (2009).
52. Lee, T. S. et al. BglBrick vectors and datasheets: A synthetic biology platform for gene expression. *J. Biol. Eng.* **5**, 12 (2011).
53. Hagen, W. R. *Biomolecular EPR Spectroscopy*. CRC Press. (CRC Press, Boca Raton, 2008).
54. Bradford, M. M. A rapid and sensitive method for the quantitation of microgram quantities of protein utilizing the principle of protein-dye binding. *Anal. Biochem.* **72**, 248–254 (1976).
55. Datsenko, K. A. & Wanner, B. L. One-step inactivation of chromosomal genes in *Escherichia coli* K-12 using PCR products. *Proc. Natl Acad. Sci. USA* **97**, 6640–6645 (2000).
56. Parker, W. L. et al. SQ 27,860, a simple carbapenem produced by species of *Serratia* and *Erwinia*. *J. Antibiot. (Tokyo)* **35**, 653–660 (1982).

Life Sciences Reporting Summary

Nature Research wishes to improve the reproducibility of the work that we publish. This form is intended for publication with all accepted life science papers and provides structure for consistency and transparency in reporting. Every life science submission will use this form; some list items might not apply to an individual manuscript, but all fields must be completed for clarity.

For further information on the points included in this form, see [Reporting Life Sciences Research](#). For further information on Nature Research policies, including our [data availability policy](#), see [Authors & Referees](#) and the [Editorial Policy Checklist](#).

Please do not complete any field with "not applicable" or n/a. Refer to the help text for what text to use if an item is not relevant to your study. For final submission: please carefully check your responses for accuracy; you will not be able to make changes later.

▶ Experimental design

1. Sample size

Describe how sample size was determined.

No sample size calculations were performed. The sample sizes used for all experiments (n = 2 or 3) in accordance with community standards.

2. Data exclusions

Describe any data exclusions.

No data was excluded from the analysis

3. Replication

Describe the measures taken to verify the reproducibility of the experimental findings.

All replication attempts in this study were successful.

4. Randomization

Describe how samples/organisms/participants were allocated into experimental groups.

All bacterial cell cultures used for each experiments were grown under the same conditions, so randomization was not relevant.
For all LC-MS analyses, the order of sample injection was randomized to eliminate confusion of experimental and temporal factors, that would interfere with data interpretation.

5. Blinding

Describe whether the investigators were blinded to group allocation during data collection and/or analysis.

This study only provides objective analytical measurements of samples derived from bacterial cultures subjected to identical growth conditions per experiment. Blinding was not relevant for this study

Note: all in vivo studies must report how sample size was determined and whether blinding and randomization were used.

6. Statistical parameters

For all figures and tables that use statistical methods, confirm that the following items are present in relevant figure legends (or in the Methods section if additional space is needed).

- | | |
|-------------------------------------|---|
| n/a | Confirmed |
| <input type="checkbox"/> | <input checked="" type="checkbox"/> The <u>exact sample size</u> (<i>n</i>) for each experimental group/condition, given as a discrete number and unit of measurement (animals, litters, cultures, etc.) |
| <input type="checkbox"/> | <input checked="" type="checkbox"/> A description of how samples were collected, noting whether measurements were taken from distinct samples or whether the same sample was measured repeatedly |
| <input type="checkbox"/> | <input checked="" type="checkbox"/> A statement indicating how many times each experiment was replicated |
| <input checked="" type="checkbox"/> | <input type="checkbox"/> The statistical test(s) used and whether they are one- or two-sided
<i>Only common tests should be described solely by name; describe more complex techniques in the Methods section.</i> |
| <input checked="" type="checkbox"/> | <input type="checkbox"/> A description of any assumptions or corrections, such as an adjustment for multiple comparisons |
| <input checked="" type="checkbox"/> | <input type="checkbox"/> Test values indicating whether an effect is present
<i>Provide confidence intervals or give results of significance tests (e.g. P values) as exact values whenever appropriate and with effect sizes noted.</i> |
| <input type="checkbox"/> | <input checked="" type="checkbox"/> A clear description of statistics including <u>central tendency</u> (e.g. median, mean) and <u>variation</u> (e.g. standard deviation, interquartile range) |
| <input type="checkbox"/> | <input checked="" type="checkbox"/> Clearly defined error bars in <u>all</u> relevant figure captions (with explicit mention of central tendency and variation) |

See the web collection on [statistics for biologists](#) for further resources and guidance.

► Software

Policy information about [availability of computer code](#)

7. Software

Describe the software used to analyze the data in this study.

MATLAB_R2017a
Microsoft Excel for Mac Version 15.32

For manuscripts utilizing custom algorithms or software that are central to the paper but not yet described in the published literature, software must be made available to editors and reviewers upon request. We strongly encourage code deposition in a community repository (e.g. GitHub). *Nature Methods* [guidance for providing algorithms and software for publication](#) provides further information on this topic.

► Materials and reagents

Policy information about [availability of materials](#)

8. Materials availability

Indicate whether there are restrictions on availability of unique materials or if these materials are only available for distribution by a third party.

No restrictions on availability apply.
Plasmids encoding the engineered carbapenem producing pathway will be available on Addgene.

9. Antibodies

Describe the antibodies used and how they were validated for use in the system under study (i.e. assay and species).

No antibodies were used in his study

10. Eukaryotic cell lines

a. State the source of each eukaryotic cell line used.

No eukaryotic cell lines were used in this study

b. Describe the method of cell line authentication used.

No eukaryotic cell lines were used in this study

c. Report whether the cell lines were tested for mycoplasma contamination.

No eukaryotic cell lines were used in this study

d. If any of the cell lines used are listed in the database of commonly misidentified cell lines maintained by [ICLAC](#), provide a scientific rationale for their use.

No eukaryotic cell lines were used in this study

► Animals and human research participants

Policy information about [studies involving animals](#); when reporting animal research, follow the [ARRIVE guidelines](#)

11. Description of research animals

Provide all relevant details on animals and/or animal-derived materials used in the study.

No animals were used in this study

Policy information about [studies involving human research participants](#)

12. Description of human research participants

Describe the covariate-relevant population characteristics of the human research participants.

This study did not involve human research participants